

AN EXAMINATION OF COOL-SEASON DAMAGING WIND EVENTS IN THE NORTHERN MID-ATLANTIC REGION

Raymond Kruczko and Alan M. Cope
NOAA/National Weather Service
Mount Holly, New Jersey

1. INTRODUCTION

Damaging “straight-line” winds (50 kts or greater) are the most common form of severe convective weather found in the northeastern U.S. and mid-Atlantic region, occurring about three times as often as large hail (.75 inch diameter or greater). About 80 percent of these severe wind events occur during the late spring and summer, i.e., May through August. The remaining 20 percent of severe wind events that occur from September through April pose a special challenge to operational meteorologists, as they often occur in weather regimes that appear only marginally favorable for development of any thunderstorms. Moreover, they are often accompanied or followed by strong, potentially damaging winds that result from intense synoptic-scale pressure gradients.

This paper will present the meteorological setting and radar signatures associated with some cool season convective wind events in the mid-Atlantic region. Mean values for severe weather parameters with these events will be contrasted with those for warm season events. Examples of various radar signatures that produced severe winds will be presented, including strong linear echoes, bowing line segments, and “broken-S” signatures. The examples will include high-resolution radar velocity data, since it often resolves structures along a convective line better than radar reflectivity. Finally, since cool season convective wind events are often embedded within larger-scale high wind regimes, the relative value of severe thunderstorm warnings vs. high wind warnings will be considered within the context of current NWS watch/warning guidelines.

2. DATA AND METHODOLOGY

The authors examined local severe weather records from 1999 to 2005 for the National Weather Service (NWS) Forecast Office in Mount Holly, NJ, as well as the National Oceanic and Atmospheric Administration (NOAA) publication *Storm Data* (NOAA 1999-2005). Eight days were identified during the months September through April on which there were five or more convective wind events (Table 1). Archived radar data for

each day were then loaded into the NWS Weather Event Simulator, along with Rapid Update Cycle, 40 km resolution (RUC-40) model analyses for the more recent events. For events before 2003 (cases 1-4 in Table 1), archived surface and upper-air data from various weather archive sites on the Internet were examined.

3. METEOROLOGICAL CHARACTERISTICS

3.1. *Similarities among the events*

These convective wind events were driven primarily by strong dynamical forcing, and were not limited to any particular time of day or night (see Table 1). However, all the tornadoes, except those in the 9/23/03 case, occurred in the more typical afternoon or early evening time frame.

Each event preceded a cold frontal passage, and most were associated with a strong, progressive surface low-pressure center to the north. Also typically present was a 250 mb jet streak core of 100 to 150 kts, oriented southwest to northeast. The events on 1/18/1999 were likely enhanced by the left front quadrant of the upper jet, while two more recent events, 9/23/2003 and 1/14/2005, were aided by the right rear quadrant.

In each case, temperatures for the date were above normal, as shown by the readings from Philadelphia International Airport (PHL) in Table 2. Even so, instability parameters remained on the low side. The air mass in which these events occurred was often just marginally unstable, with Convective Available Potential Energy (CAPE) usually less than 500 Jkg⁻¹. Two cases were a little out of the norm. The 9/23/2003 events had CAPE values approaching 1000 Jkg⁻¹, while the 10/15/2003 events were on the opposite end of the spectrum with values less than 100 Jkg⁻¹.

The typical large-scale meteorological setting for these cool-season events is illustrated in Fig 1. This figure shows a composite of parameters for all eight cases, constructed with data from the NCEP/NCAR reanalysis project (Kistler, et.al., 2001), accessed via the web-based interface at <http://www.cdc.noaa.gov/Composites/Hour>. A mean upper-level jet streak is found to the west, from the central Appalachians northward into Ontario (Fig 1a), and a strong mid-level trough

Corresponding author address: Raymond Kruczko,
NOAA National Weather Service, Mount Holly, NJ;
e-mail: Raymond.kruczko@noaa.gov

axis extends across the Great Lakes and Ohio Valley (Fig 1b). A well-defined low-level moist axis extends northward along the Atlantic Coast (Fig 1c), while the surface pressure trough associated with the cold front lies just to the west (Fig 1d).

Meteorological upper-air fields from each event were also compared with climatological normals from the NCEP/NCAR re-analysis (Hart and Grumm, 2001), again using a web-based interface at <http://hart.met.psu.edu/meteo497/mapper.html>. Total wind speed for each case was found to be 1-2 standard deviations (STD) above normal at 850 and 700 mb, but near normal at higher levels. However, the v-component wind was 1-2 STD above normal at all levels (850, 700, 500, 250 mb). Precipitable water was at least 2 STD above normal in all eight cases, as was specific humidity up to 500 mb for all cases except case 2. Temperatures aloft were above normal for the four winter cases (Dec., Jan., Feb.), but near normal for the others. Thus in general, it appears the most distinguishing characteristics of these cool-season events are above-normal moisture and a strong southerly wind component.

Another common factor is that very little cloud-to-ground lightning was detected with these cool season storms. Where lightning data was available (cases 5-8), 21 total cloud-to-ground strikes was the highest value recorded during any case. Van den Broeke, et.al. (2004) also noted a strong correlation between the lack of cloud to ground lightning and weak instability associated with cool season damaging wind event. Weak instability is likely also the reason no large hail was reported during any of the cool season cases in this study.

3.2 Comparison with warm season events

Numerous studies of severe convective windstorms have been made, notably Johns and Hirt (1987) and Przybylinski (1995). Recently, Burke and Schultz (2004) looked specifically at cool-season bow echoes; however, none of their cases extend much into the mid-Atlantic region. In this section, we will compare some of our findings with typical squall-line/bow-echo environments for both cool- and warm-season events, as summarized by (Funk, 2004). As noted above, strong, progressive surface low pressure systems are more associated with cool season events than warm season events. Surface convergence can be strong in both seasons. Higher than average dewpoints are common, with the greatest values in the warm season. Warm season events are often located along or north of an east-west frontal boundary, while cool season events typically occur in the warm sector along or east of a cold front. The latter was certainly true

for the events included in this paper. All were ahead of a cold front, and seven out of eight cases showed a warm front to the north.

Comparing upper-air fields, Funk (2004) states that cool season events possess moderate to strong wind fields throughout the atmosphere. 850 mb wind speeds of 30-60 kts are common, while an upper level jet stream axis aloft is nearby to the northwest (see Fig. 1a). Synoptic winds in general tend to be stronger than warm season events. All of our cases displayed strong winds fields, as can be inferred from the shear and helicity values in Table 2, and the cell velocities in Table 3. Significant divergent/convergent fields aloft and dynamical forcing are more associated with cool season events. This is needed to overcome the limited amount of moisture and instability usually found within the system. Environmental wind momentum aloft may transfer downward causing damaging surface winds, especially if no low-level inversion is present. For several cases in our study, it is likely that the momentum transfer process did in fact lead to surface damage.

Comparing the thermodynamic and vertical wind shear profile, Funk (2004) notes that cool season events contain less instability than warm-season events. CAPE values during cool season events are commonly between 500 and 2000 J/kg. Warm season events correspond with CAPE values typically between 2000 and 4500 J/kg. Table 2 suggests that our cases were below or on the lower end of the cool-season range for CAPE. Cool season events are associated with moderate to strong ($>25 \text{ ms}^{-1}$) shear within the lowest 2.5 km, similar to warm season events. For the cases in our study, 0-3 km shear values (Table 2) ranged from about 15 ms^{-1} to 40 ms^{-1} , averaging just over 25 ms^{-1} .

4. RADAR SIGNATURES

Table 3 lists some of the radar characteristics of the cool-season cases in this study. Radar signatures observed during cool season events varied from nearly solid lines of 50 dBZ or greater to short bow echoes or broken-S type signatures to isolated cells. Most typical were nearly solid 30-35 dBZ lines with embedded higher values. Cell movement was very rapid, usually 50 kts or greater. Storm-echo tops were relatively low, typically less than 8 km. In some cases they were as low as 5 km and in some as high as 11 km. Maximum vertically integrated liquid (VIL) was relatively low, ranging from as little as $15\text{-}20 \text{ kgm}^{-2}$ up to $35\text{-}40 \text{ kgm}^{-2}$.

The rapid speed of the cells was likely enough to contribute to wind damage in some events. Also, damage reports, as can be expected, often lined

up well with bowing segments. Another common damage-related area, either from straight-line or rotational winds, was where line segments split (Figs. 6, 7). Of the ten total tornados or waterspouts (from four of the eight cases), at least six seemed to occur near a split or break in a convective line segment.

As might be expected, each case in this study exhibited a unique combination of radar signatures. Specifically, during the 18 January 1999 case, the second (trailing) line of convection associated with the cold front carried a greater amount of damaging winds than the pre-frontal trough, although the highest radar reflectivity was associated with the trough (Fig. 2). During the December 17th, 2000 event, bow echoes were observed in reflectivity patterns, but not in velocity patterns (Fig. 3). The mean flow was strong enough, in this case, to obscure any velocity discontinuity signatures. With the 23 September 2003 event, reflectivity data were less valuable than the velocity data. There were no discernable hooks in the reflectivity data associated with the four tornadoes that occurred that day (Figs. 4, 5), although one could infer by the bowing segment that book-end vortices were possible. The 15 October 2003 event had evidence of both storm-related wind damage and synoptic-related wind damage. The KDOX image (Fig. 6, upper panels) clearly showed strong winds behind a bowing segment. During the same event (approximately 1 1/2 hour later), the KDIX image (Fig. 6, lower panels) showed a strong southerly flow ahead of the squall line. Damage associated with this feature was due to these strong winds mixing down to the surface. The 14 January 2005 event (Figs. 7,8) showed a broken-"S" type signature, known to be associated with wind damage (as in this case) and also tornadoes (McAvoy, et al., 2000).

5. CONCLUDING DISCUSSION

Cool season wind events are no different than events at other times of year in terms of offering challenges to the radar-warning meteorologist. For example, not only does he/she have to be concerned with winds generated by a storm itself, but also with strong environmental or synoptic winds which may also be present. A review of Storm Data indicated that five of the eight cases in this study also included non-thunderstorm wind-damage entries (see Table 1).

These cases show that one cannot rely on a single specific radar parameter during cool-season events; rather, a well-balanced interrogation is needed. In some of the cases, reflectivity images implied wind damage was possible while velocity data did not. In other

cases, velocity proved to be the more useful parameter.

Besides a well-balanced interrogation, the warning meteorologist is also tasked with issuing the product(s) that best accommodates the situation. This can be challenging with cool season events due to the characteristics they exhibit. When the threats of both convective-initiated winds and synoptic winds are intermixed, choosing between a Severe Thunderstorm Warning (SVR), Wind Advisory/High Wind Warning, or a combination of both, can be difficult. The meteorologist must ask which product makes more sense to the end users. If he/she chooses to issue the SVR, how will the public react to events that contain little if any lightning? The relative lack of lightning (and thunder) could be an additional danger, if the public believes thunder will precede or accompany the severe weather threat. Absence of thunder might lead to the conclusion that the threat is over or is not going to materialize.

High Wind Warnings (NPW) are usually associated with synoptic-scale events lasting one hour or longer. However, the individual wind events in the cases described in this paper are generally much shorter. When convection is embedded within an intense synoptic-scale wind regime, will a SVR issuance "on top of" a pre-existing NPW serve to clarify or confuse the public? These challenges also affect Storm Data and national verification, where distinctions need to be made between convective and non-convective events (often well after the events are over). In the NWS Eastern Region, some guidance has been provided for dealing with combined synoptic and mesoscale events (NOAA/NWS 1998). While this paper does not attempt to offer solutions to the questions raised above, it is believed they are worthy of further study and discussion.

6. REFERENCES

- Burke, P.C. and D.M. Schultz, 2004: A 4-yr climatology of cold-season bow echoes over the continental United States. *Wea. Forecasting*, **19**, 1061-1074.
- Funk, T., 2004 (cited 2005): Structure and evolution of squall line and bow echo convective systems. [Available online at <http://www.crh.noaa.gov/lmk/soo/docu/bowecho.htm>].
- Hart, R.E., and R.H. Grumm, 2001: Using normalized climatological anomalies to rank synoptic-scale events. *Mon. Wea. Rev.*, **129**, 2426-2442.

Johns, R.H. and W.D. Hirt, 1987: Derechos: Widespread convectively induced windstorms. *Wea. Forecasting*, **2**, 32-49.

Kistler, R., E. and co-authors, 2001, The NCEP-NCAR 50-year reanalysis: monthly means CD-ROM and Documentation. *Bull. Amer. Soc.*, **82**, 247-267.

McAvoy, B.P., W.A. Jones, and P.D. Moore, 2000: Investigation of an unusual storm structure associated with weak to occasionally strong tornadoes of the eastern United States. Preprints, 20th Severe Local Storms Conference, Orlando, FL, Amer. Meteor. Soc., 182-185.

NOAA, 1999-2005: Storm data and unusual weather phenomena. National Climatic Data Center, Ashville, North Carolina. [Available online at <http://www.ncdc.noaa.gov>].

NOAA/NWS, 1998: High wind outlooks, watches, warnings and wind advisories. Regional Operations Manual Letter E-8-98. Available from National Weather Service Eastern Region, Bohemia, New York, 11716.

Przybylinski, R.W., 1995: The bow echo: Observations, numerical simulations, and severe weather detection methods. *Wea. Forecasting*, **10**, 203-218.

Van Den Broeke, M.S., D.M. Schultz, R.H. Johns, J.S. Evans, and J.E. Hales, 2004: Cloud-to-Ground Lightning Production in Strongly Forced, Low-Instability Convective Lines Associated with Damaging Winds. Submitted as an article to *Weather and Forecasting*.

Table 1. Cool-season severe weather events in this study.

Case No.	Date	Time (UTC)	Convective Wind Events	Tornados	Synoptic Scale Wind Events
1	01/18/1999	2000 to 2200	5	2	13
2	02/12/1999	1900 to 2400	5	1	1
3	12/17/2000	1300 to 1800	10	0	4
4	03/10/2002	0500 to 0900	10	0	5
5	09/23/2003	1000 to 1400	18	4	0
6	10/15/2003	0200 to 0500	16	0	4
7	10/27/2003	1900 to 2200	12	3	0
8	01/14/2005	0900 to 1100	11	0	0

Table 2. Some meteorological parameters for cases in this study. Temperature departures from normal are based on 1971-2000 data.

Case No.	Max/Min Temperature at PHL (deg F)		Shear 0 to 3 km (ms^{-1})	Helicity 0 to 3 km (m^2s^{-2})	CAPE (Jkg^{-1})
	Obs.	Departure			
1	55/38	+17/+13	29.7	663	<200
2	57/43	+16/+16	27.9	430	<400
3	57/50	+13/+20	39.3	553	<300
4	65/32	+16/ -01	26.4	558	<400
5	79/64	+04/+06	14.7	380	<1000
6	71/51	+05/+02	22.2	505	<100
7	70/62	+08/+17	22.8	260	<400
8	66/37	+27/+12	24.3	600	<400
Avg.	65/47	+13/+11	25.9	494	<400

Table 3. Radar characteristics of events in this study.

Case No.	Typical Echo Tops (kft)	Maximum VIL (kg m^{-2})	Mean Cell Velocity (from deg/kt)	Line Motion (kts)	Echo Signature
1	20-25	35-40	215/60	E 40	two lines, broken segments
2	15-20	20-25	225/50	E 30	short line segments
3	20-25	35-40	205/70	E 30	multiple segments, some bowing
4	30-35	35-40	230/50	E 20	solid line, breaking into segments
5	20-25	30-35	210/45	E 25	broken segments, short bows
6	30-35	25-30	210/55	E 35	bowing segments, broken "S"
7	25-30	25-30	220/45	E 30	cells embedded in weaker line
8	20-25	15-20	225/55	E 25	solid line, broken "S"
Avg.	22-27	27-32	217/54	E 29	N/A

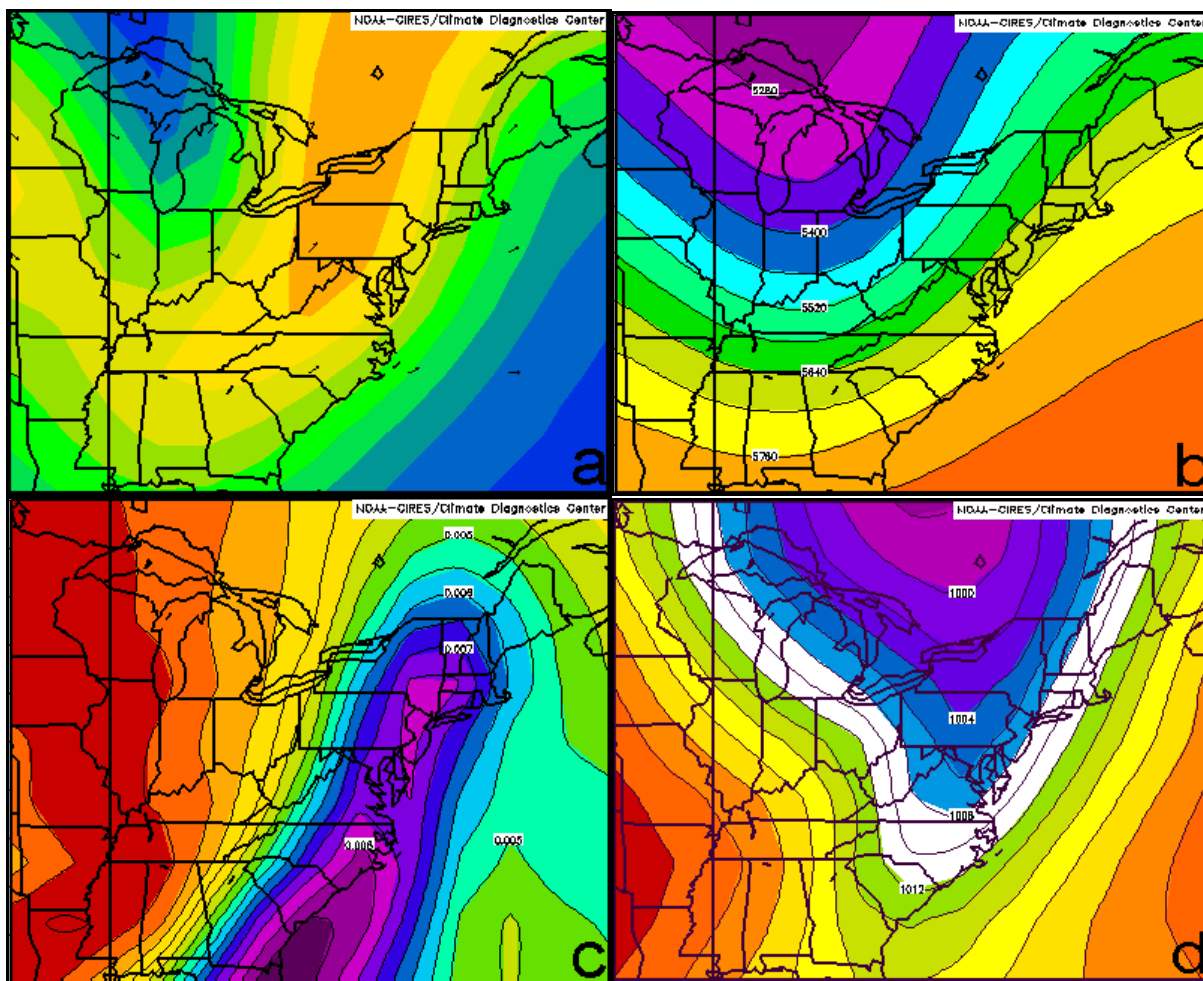


FIG 1. Mean composite fields for the eight cases in this study, derived from the NCEP/NCAR reanalysis project: (a) 250mb winds (ms^{-1} , orange is 50+); (b) 500mb heights (m); (c) 850mb specific humidity (gg^{-1}); (d) mean sea-level pressure (mb). Analysis time used for each case is the six-hourly UTC time (00,06,12,18) nearest the first severe event.

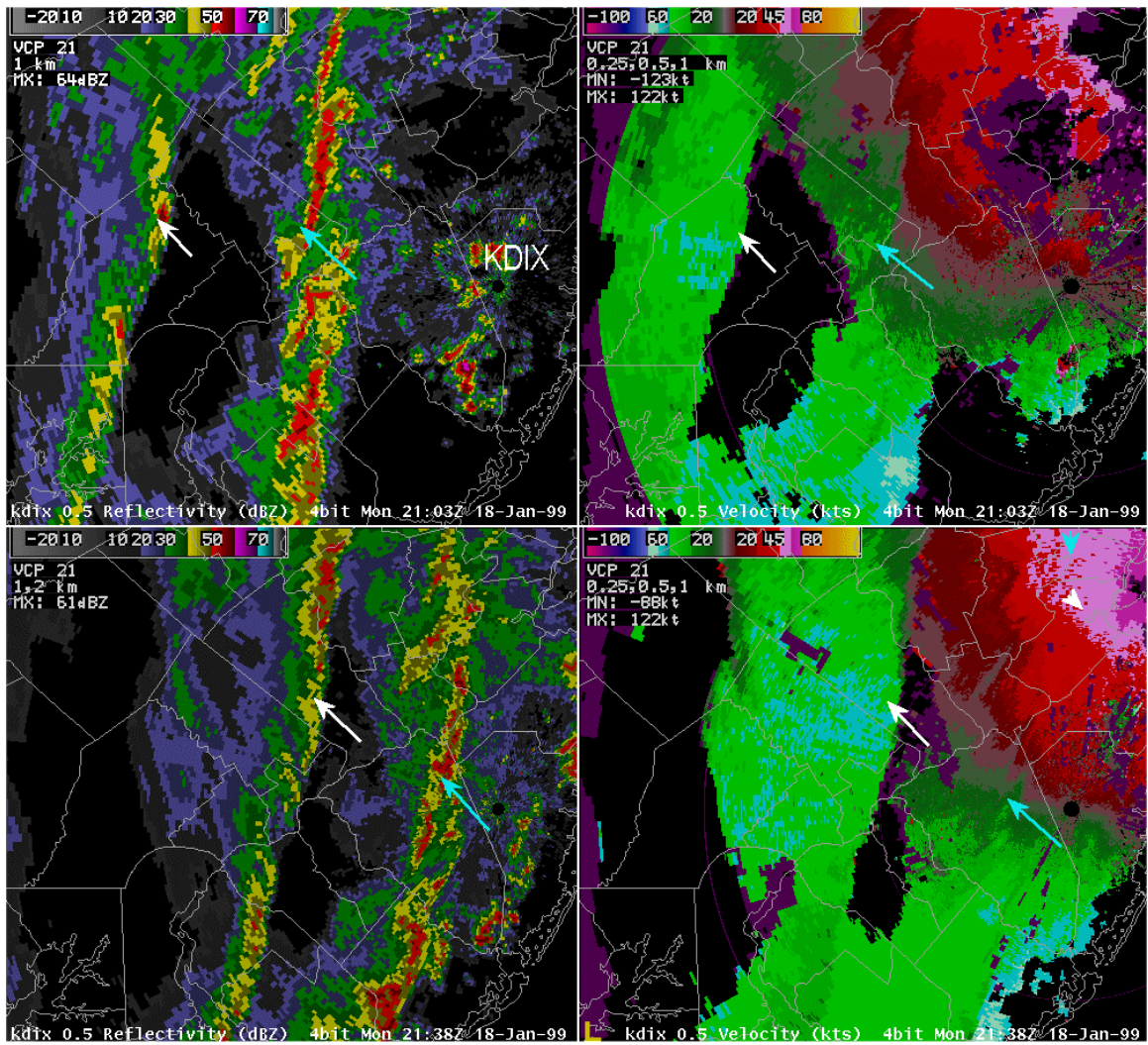


FIG 2. KDIX radar 16-level data at 0.5 deg elevation for case 1, 18 January 1999. Upper left: base reflectivity at 2103 UTC. Upper right: corresponding base velocity. Lower left: base reflectivity at 2138 UTC. Lower right: corresponding base velocity. Blue arrows indicate pre-frontal convection with stronger reflectivity. White arrows indicate frontal convection followed by stronger inbound velocity. KDIX is the radar location.

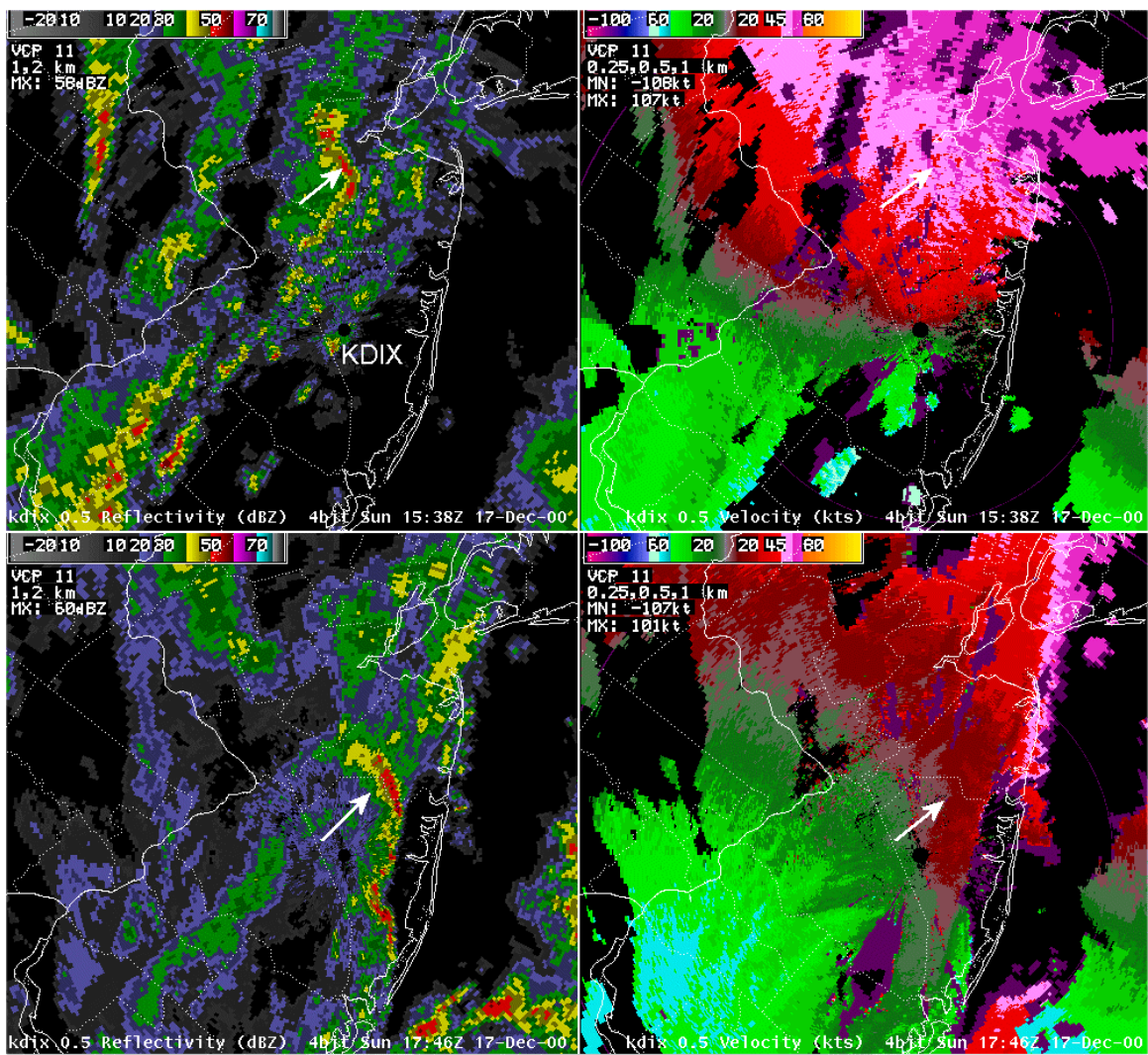


FIG 3. Same as Fig 2, except for case 3, 17 December 2000, at 1538 UTC (upper panels) and 1746 UTC (lower panels). White arrows indicate locations of bow echo features.

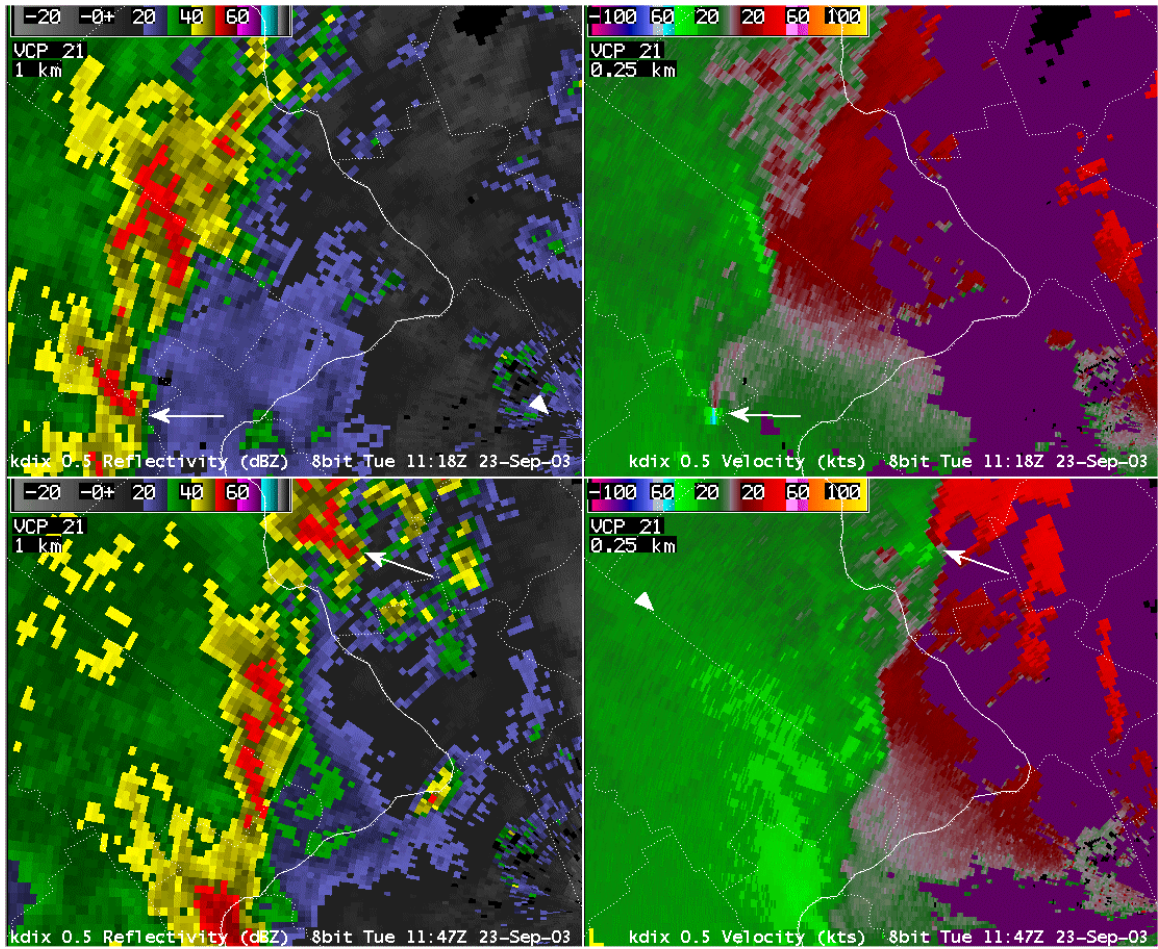


FIG 4. Same as Fig 2, except higher resolution (256-level) data for case 5, 23 September 2003, at 1118 UTC (upper panels) and 1147 UTC (lower Panels). White arrows indicate the locations of tornadoes occurring around the time of the image. The KDIX radar is just off the SE corner of each image.

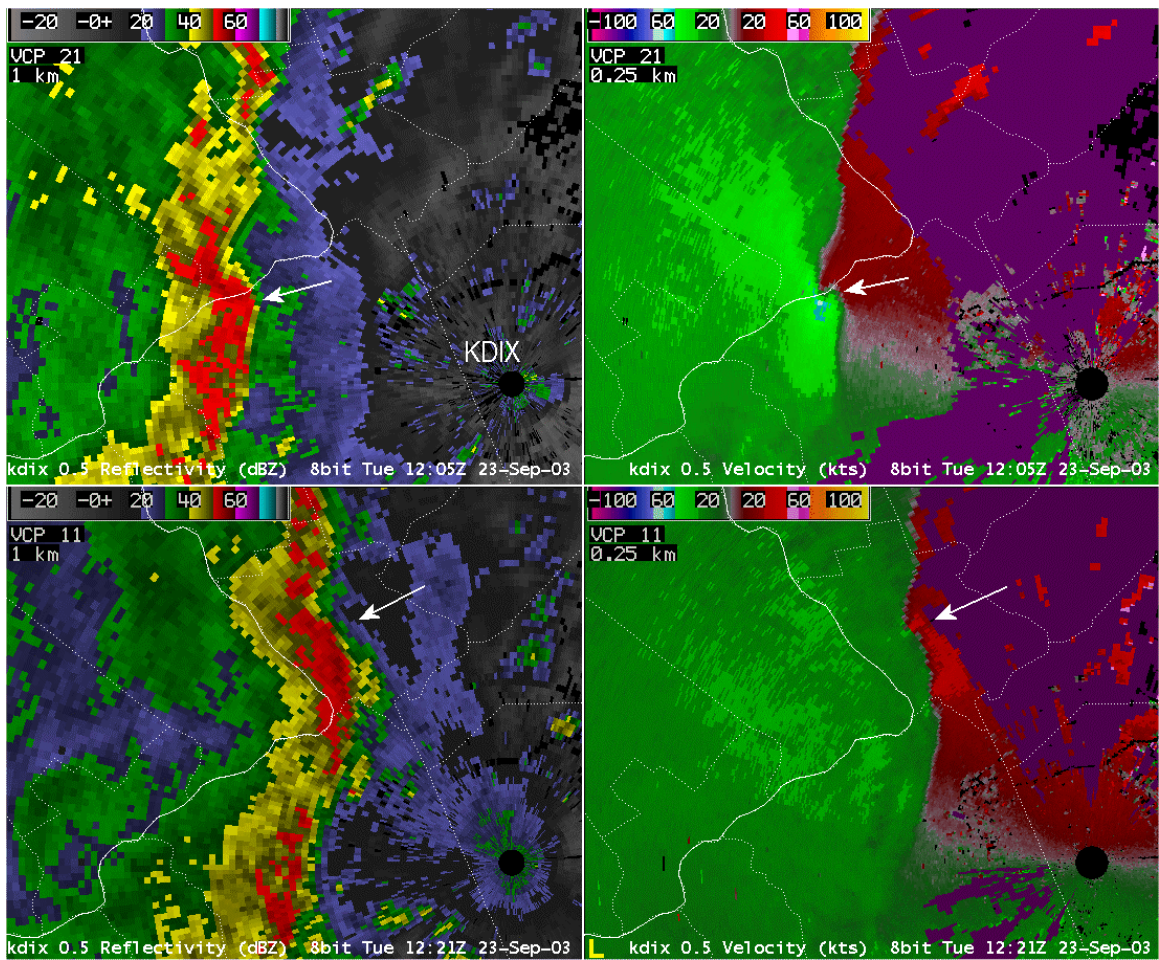


FIG 5. Same case as Fig 4, except at 1205 UTC (upper panels) and 1221 UTC (lower panels). White arrows indicate locations of tornadoes.

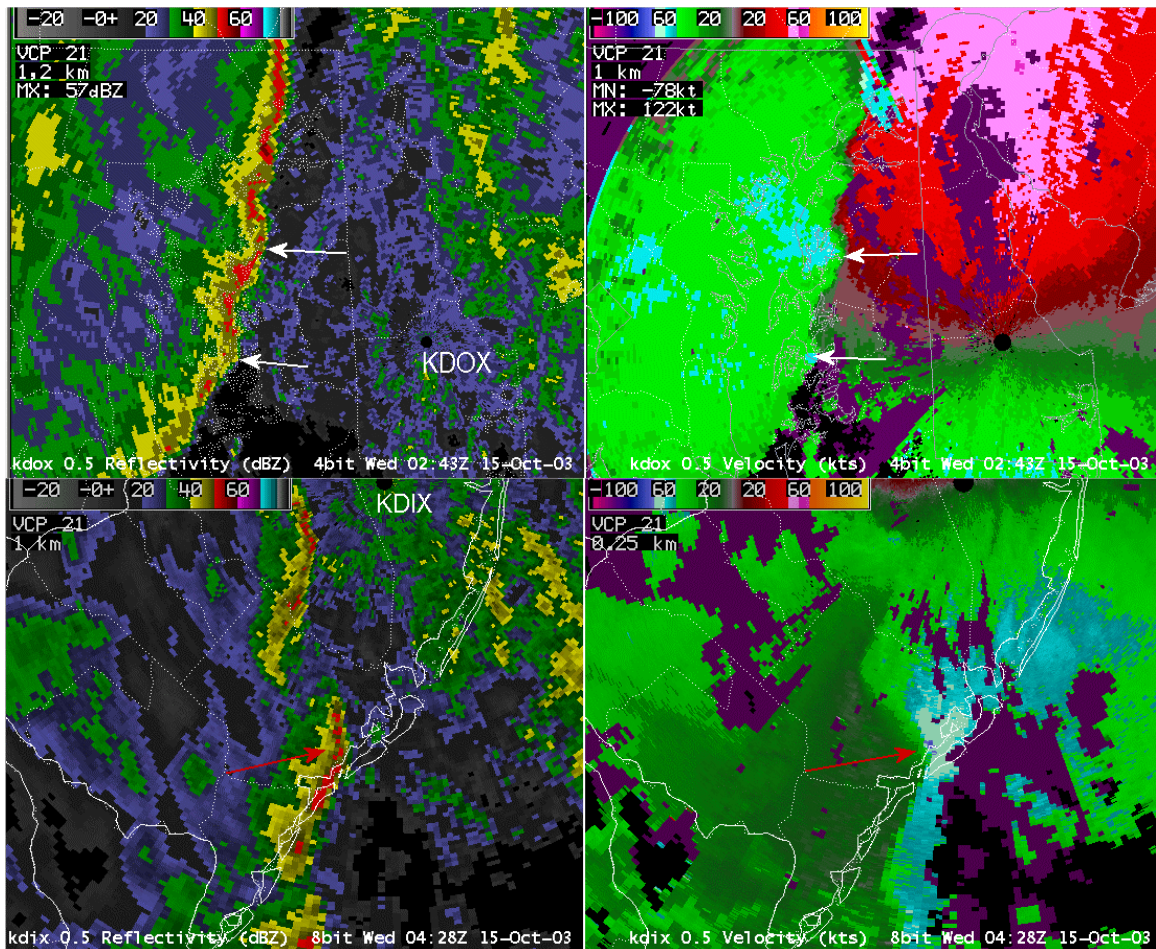


FIG 6 KDOX (Dover AFB) radar 16-level base reflectivity data for case 6, at 0243 UTC on 15 October, 2003 (upper left), and corresponding base velocity (upper right). KDIX radar 256-level base reflectivity data at 0428 UTC, same day (lower left) and corresponding base velocity (lower right). White arrows in upper panels indicate bowing-line segments associated with in-bound wind maxima. KDOX is the location of the Dover AFB radar. Red arrows in lower panels indicate the southern half of a "broken-S" signature, where mid-level winds of nearly 80 kts have mixed down to 2800 ft MSL.

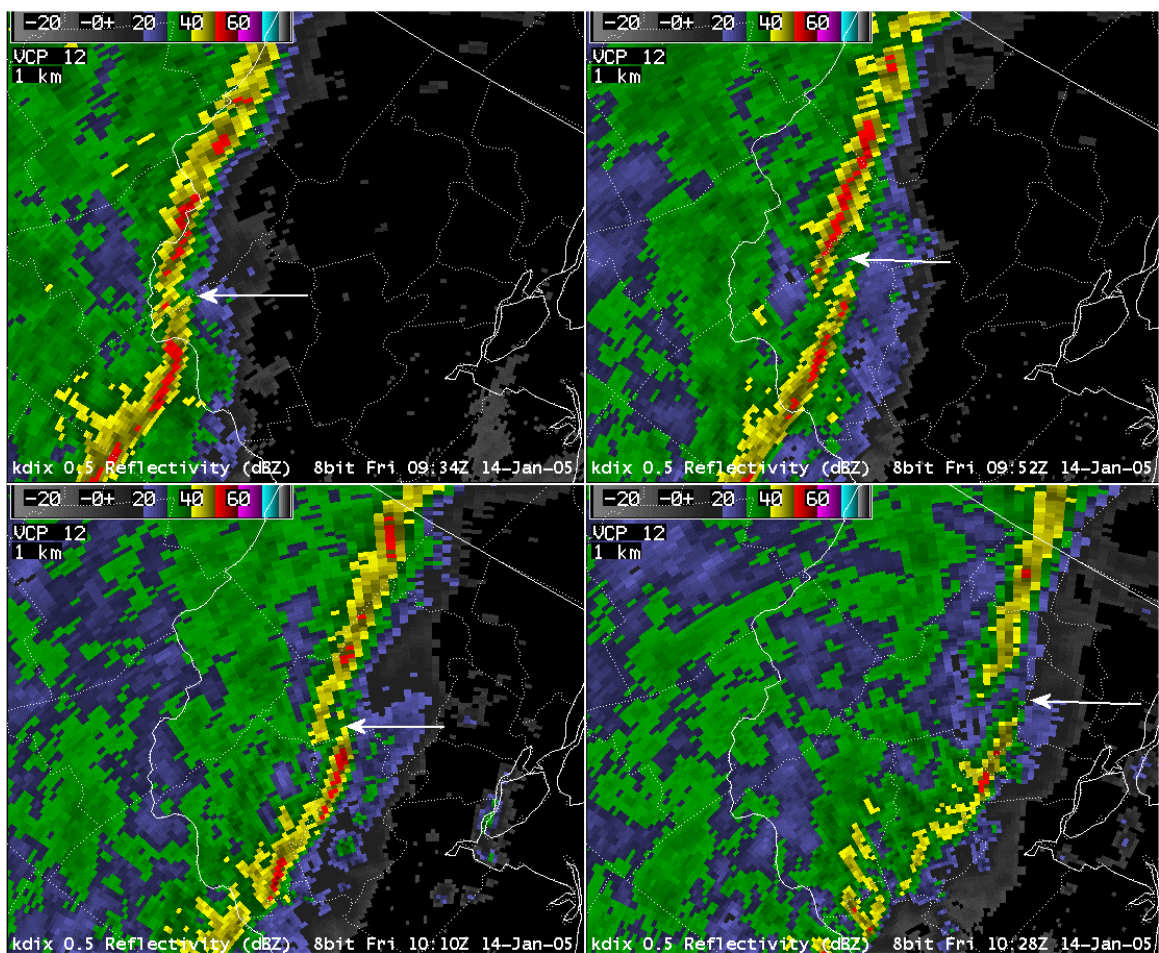


FIG 7 KDIX radar 256-level base reflectivity data at 0.5 deg elevation for case 8, 14 January, 2005, at 0934 UTC (upper left), 0952 UTC (upper right), 1010 UTC (lower left) and 1028 UTC (lower right). White arrows indicate location of “broken-S” feature. The KDIX radar is to the SE of each image.

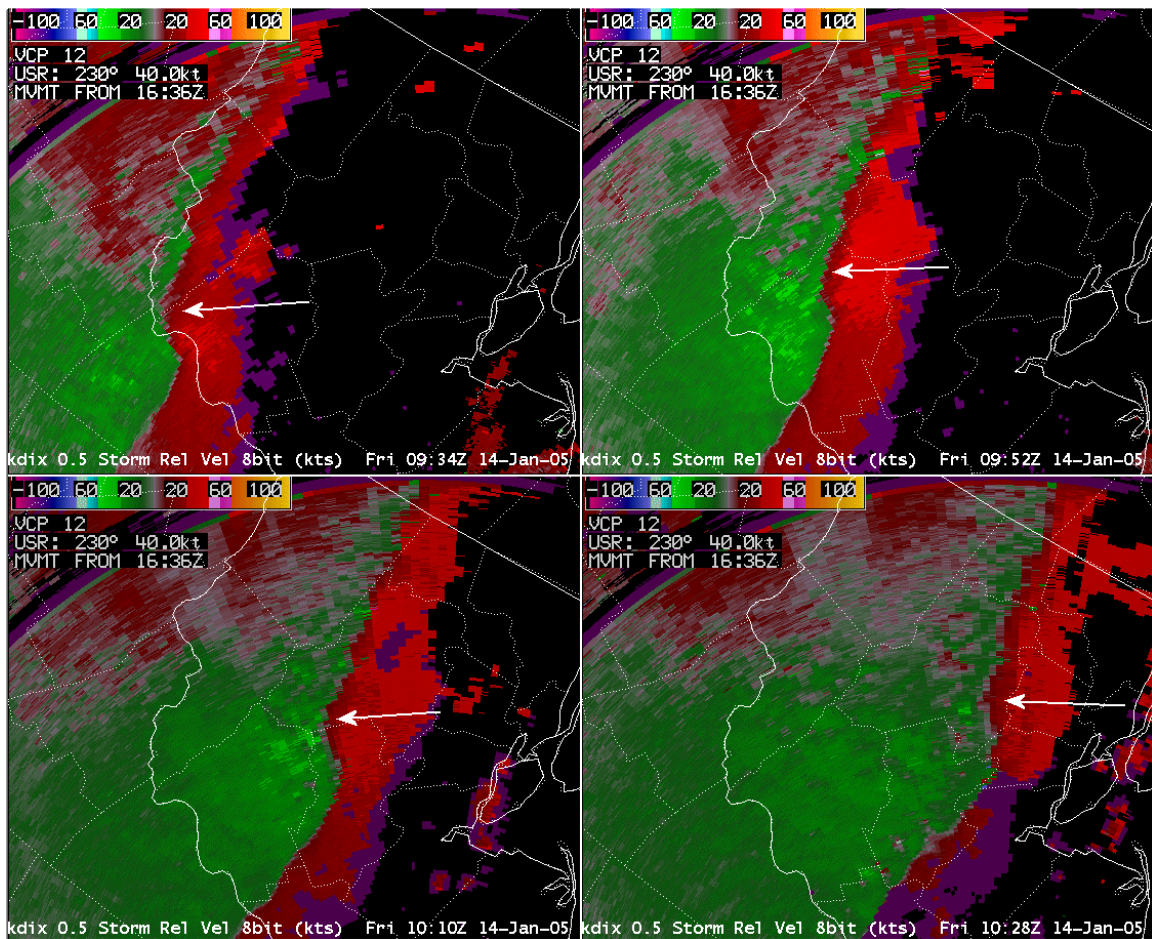


FIG 8. Same as Fig 7, except base velocity data at corresponding times.